Check for updates

View Article Online
View Journal

Journal of
Materials Chemistry B

Materials for biology and medicine

Accepted Manuscript

This article can be cited before page numbers have been issued, to do this please use: H. Li, Y. Hao, W. Feng and Q. Song, *J. Mater. Chem. B*, 2020, DOI: 10.1039/D0TB01784A.

This is an Accepted Manuscript, which has been through the Royal Society of Chemistry peer review process and has been accepted for publication.

Accepted Manuscripts are published online shortly after acceptance, before technical editing, formatting and proof reading. Using this free service, authors can make their results available to the community, in citable form, before we publish the edited article. We will replace this Accepted Manuscript with the edited and formatted Advance Article as soon as it is available.

You can find more information about Accepted Manuscripts in the Information for Authors.

Please note that technical editing may introduce minor changes to the text and/or graphics, which may alter content. The journal's standard Terms & Conditions and the Ethical guidelines still apply. In no event shall the Royal Society of Chemistry be held responsible for any errors or omissions in this Accepted Manuscript or any consequences arising from the use of any information it contains.

ROYAL SOCIETY OF CHEMISTRY

rsc.li/materials-b

View Article Online
DOI: 10.1039/D0TB01784A

ARTICLE

Rapid and sensitive detection of nitric oxide by a BODIPY-based fluorescent probe in live cells: Glutathione effects

Hao Li, Yu-Hao Hao, Wei Feng and Qin-Hua Song*

Received 00th January 20xx,
Accepted 00th January 20xx

DOI: 10.1039/x0xx00000x

Nitric oxide (NO) is an important signaling molecule involved in various physiological and pathological processes. The effects of NO depend on its concentration, spatial and temporal constraints of the cell microenvironment. Meanwhile, NO can react with some biomolecules such as biothiols, leading to a short biological lifetime. Thus, it is very crucial to establish a real-time visualization method for monitoring NO levels. In this work, we have developed a fluorescent probe RBA for NO, with a 3-extended BODIPY as a fluorophore and a secondary amine as the active site. The probe RBA can fast sense NO (~10 s) in aerobic solutions to generate a fluorescent N-nitrosamine (RBA-NO, Φ_f = 0.87) due to blocking the photo-induced electron transfer (PET) process from the secondary amine to BODIPY core. This sensing reaction displays high sensitivity (LOD =10 nM), and high selectivity for NO over relevant analytes except some reducing reagents including biothiols exhibit a remarkable interference effect ascribing to competition reaction for biothiols. Furthermore, the exo- and endogenous detections of NO in live cells and zebrafish were achieved, and it was demonstrated that glutathione (GSH) weakens drastically the fluores-cence response by cell-imaging experiments. These results imply that colorimetric and fluorescent response of the chemosensor for NO depends the levels of both NO and GSH in environments.

Introduction

Nitric oxide (NO), biosynthesized by nitric oxide synthase (NOS) or generated from nitrite under hypoxic or acidic conditions, plays key roles in numerous processes such as the regulation of vascular tone, neuronal signaling, immunology.[1] The effects of NO depend on its concentration, and spatial and temporal constraints of the cell microenvironment. The abnormal level of NO production is implicated in a large number of pathological processes such as cancer, the endothelial dysfunction, and neurodegenerative diseases.[2] For this reason, enormous efforts have been made to develop sensitive and selective methods to detect NO concentration and distribution in living cells.[3]

In contrast to other NO imaging techniques,[4] the fluorescence imaging has many advantages such as high sensitivity, high selectivity, high spatio-temporal resolution, and noninvasive detection. Therefore, various fluorescent probes for NO have been designed in the past two decades,[5] and most fluorescent probes can be classified into two main types: one is based on o-diamino aromatics,[6] initiated by Nagano's group, and another is based on metal-ligand complexes,[7] pioneered by Lippard's group.

In current years, some new strategies have been developed, for instance, pioneer works including the nitrosation reaction with secondary amine,[8] the formation of diazo ring from o-amino-3'-dimethylaminophenyl aromatics,[9] reductive deamination of aromatic primary monoamines,[10] aromatization of the Hantzsch ester,[11] the formation of Se-NO bond,[12] and others.[13] The pioneer works and subsequent works allow diverse chemical detections of NO in solutions and live cells. For example, *N*-nitrosation as the sensing reaction between a secondary amine and NO/O_2 generates a nitrosamine, giving a turn-on fluorescence response via blocking a photo-induced electron transfer (PET) process or switching a new intramolecular charge transfer (ICT) process.[8, 14] These amine-based fluorescent probes have wide range of response times from several seconds[8, 14d] to 20 min.[14f]

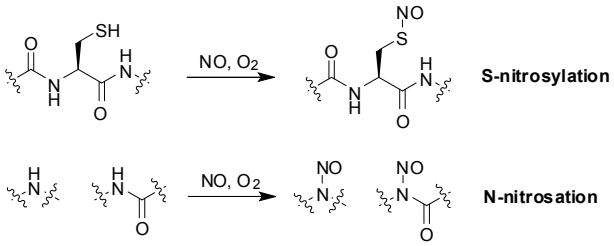

Fig. 1 *S*-nitrosylation of cysteine or glutathione and N-nitrosation of secondary amines or amides with NO in aerobic conditions.

In aerobic organisms, NO can fast react with some active biomolecules such as glutathione (GSH) and cysteine (Cys) to form a *S*-nitrosothiol (SNO), or secondary amines and amides to form *N*-nitrosocompounds,[15] leading to a short biological half-life (0.05–1 s),[16] shown in Fig. 1. Thus, the sensing reaction of NO and a probe is in competition with the reactions of biomolecules, that is, a fast sensing reaction could achieve real-

Department of Chemistry, University of Science and Technology of China, Hefei 230026, P. R. China. E-mail: qhsong@ustc.edu.cn

† Electronic Supplementary Information (ESI) available: Photostability of RBA and its sensing product, MS evidence of reaction products of RBA or GSH with NO, DFT calculations for PET process, GSH effects on the sensing reaction, cytotoxicity, fluorescence intensity from imaging of NO in live cells, and copies of NMR spectra of new compounds.. See DOI: 10.1039/x0xx00000x

Published on 19 September 2020. Downloaded by University of Rochester on 9/19/2020 4:01:35 PM.

Journal of Materials Chemistry B Accepted Manuscript

View Article Online
DOI: 10.1039/D0TB01784A

Published on 19 September 2020. Downloaded by University of Rochester on 9/19/2020 4:01:35 PM.

time detection of NO, and a slow sensing reaction may not start until the reactions of active biomolecules with NO have completed. Hence, the rapid response is very necessary for a fluorescent probe for the real-time detection of NO.

Intracellular GSH is the most abundant biothiol, with a concentration of mM (1-10 mM), and NO can rapidly react with GSH to form S-nitrosoglutathione (GSNO).[17] Thus, S-nitrosylation of GSH should be the most competitive reaction to the sensing reaction. So far, there are several papers that reported effects of biothiols on the sensing behavior toward NO in the selectivity experiments.[8, 12, 18] The results show small effects or even no effect on the response of a probe toward NO, and seem independent on the response time of the probe toward NO. For instance, little decrease in response fluorescence intensity in the presence of biothiols was found for the systems with the most rapid response (for example, 10 s for 4 μM probe toward 24 μM NO),[8, 18f] and no effect for the systems with long response times (such as 15 min for 20 μM probe toward 100 μM NO).[12, 18c] Moreover, there is no report about GSH effects on the chemical detection of NO in live cells.

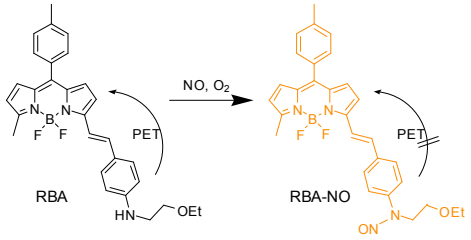

Scheme 1. The structures of the probe RBA and its sensing reaction between NO

In this work, we have constructed such a fluorescent probe with 3-extended BODIPY as a fluorophore and secondary amine as active group, RBA, shown in Scheme 1. RBA can fast sense NO in aerobic condition to form a N-nitrosamine, RBA-NO, giving a turn-on fluorescence response, which can be decreased by biothiols and antioxidants in solutions. Moreover, the sensing behavior of RBA has been observed from fluorescence imaging of NO at different levels of GSH in live cells and zebrafish.

Results and discussion

Synthesis of the probe and its conversion

The synthetic route of the probe was outlined in Scheme 2. Briefly, 4-vinylaniline as a starting material was N-alkylated in the presence of 1-bromo-2-ethoxyethane to form compound **1**. Then, the amino group of **1** was protected with $(Boc)_2O$ to give compound **2**. Third, the double bond of **2** was oxidized with O_3 as aldehyde group, and then the protective group was removed to yield the aldehyde **3**. Finally, the aldehyde **3** reacts with the BODIPY[19] via Knoevenagel condensation to afford the target product RBA.

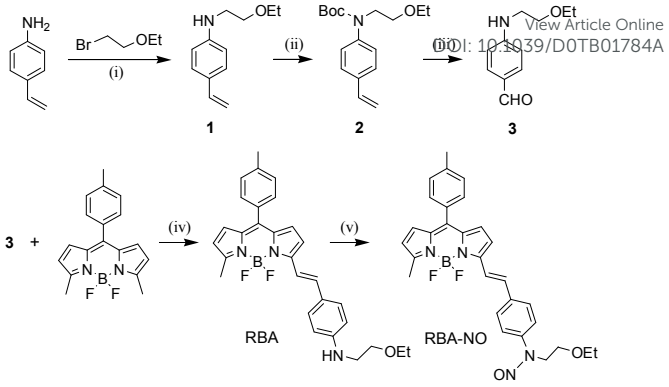

Scheme 2. Synthetic route for the probe and its conversion. Reagents and conditions: (i) 1-bromo-2-ethoxyethane, K_2CO_3, DMF, 80°C, 12 h, 40%. (ii) $(Boc)_2O$, dioxane, 85°C, 14 h, 92%. (iii) a) O_3, DCM, -78°C, Me_2S, 0.5 h; b) CF_3COOH, DCM r.t., 8 h, 30%. (iv) toluene, piperidine, TsOH, 145°C, 12 h, 37%. (v) NO aqueous solution, EtOH, r.t., 5 min, 60%.

Under NO aerobic aqueous condition, the probe RBA is converted into a N-nitrosamine, RBA-NO, as the proposed sensing product. All new compounds **1-3**, RBA and RBA-NO, were fully characterized by ^1H NMR, ^{13}C NMR and high resolution mass spectroscopy (HRMS).

Photophysical properties of RBA and its product RBA-NO

Photophysical property. The UV/Vis absorption and fluorescence spectra of the probe RBA and its sensing product RBA-NO were determined in an aqueous solution (PBS:EtOH v/v 65:35, 0.1 M PBS buffer, pH 7.4). As shown in Fig. 2, RBA displays a maximum absorption band centred at 605 nm, and its product exhibits a characteristic maximum absorption band centered at 572 nm. For emission property, the probe RBA is almost non-fluorescent (Φ_f < 0.002, see below) possibly due to a PET process from the amine to BODIPY core, and RBA-NO emits yellowish red fluorescence with a peak at 585 nm due to blocking the PET process (Fig. 2). Irradiation experiments display excellent photostability for both RBA and its sensing product RBA-NO shown in Fig. S1. The quantum yield of RBA-NO was determined to be 0.87 with cresyl violet (Φ_f = 0.54[20] in methanol) as a reference. Hence, if the probe RBA in aerobic aqueous solutions can convert into RBA-NO upon encountering NO, a turn-on fluorescence response would be observed.

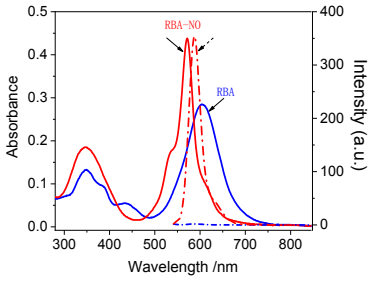

Fig. 2 UV/Vis absorption (solid) and fluorescence (dash) spectra (λ_{ex} = 530 nm) of 5 μM RBA (blue) or 5 μM RBA-NO (red) in the PBS/EtOH (v/v 65:35) solution.

Journal of Materials Chemistry B Accepted Manuscript

This journal is © The Royal Society of Chemistry 20xx

Please do not adjust margins

View Article Online DOI: 10.1039/D0TB01784A

Published on 19 September 2020. Downloaded by University of Rochester on 9/19/2020 4:01:35 PM.

Spectral response of RBA toward NO

As expected, UV/vis absorption spectra of the RBA solutions reveal the converted process from RBA to RBA-NO upon addition of NO (0-40 μM). As shown in Fig. 3a, the absorption spectra display a decrease in the absorption peak at 605 nm and appearance of a new peak at 572 nm with an isobestic point at 580 nm. Meanwhile, fluorescence spectra display a turn-on fluorescence centred at 585 nm (Fig. 3b), and the fluorescence color is yellowish red (Inset of Fig. 3b).

Based on above fluorescence titration experiment, a good linear relationship was obtained from the plot of the fluorescence intensity vs. the concentration of NO (0-15 μM) (Fig. 3c). Thus, the limit of detection (LOD) was obtained as 10 nM in terms of the equation LOD = 3σ/k, where σ is the standard deviation of blank measurement and k is the slope of the fitting straight line.

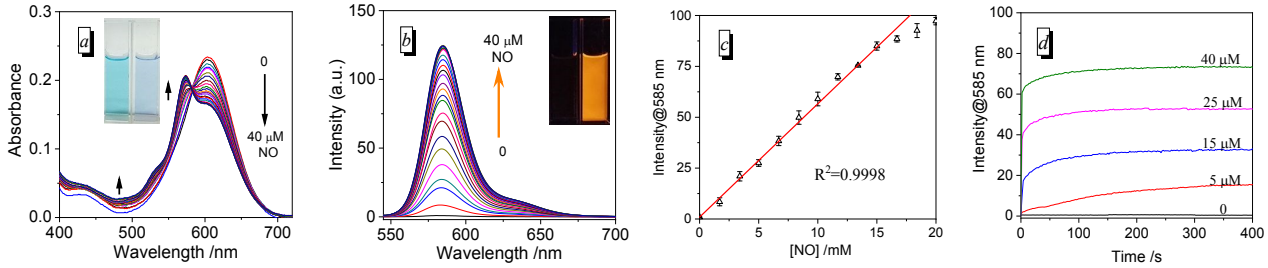

Fig. 3 (a) UV/Vis absorption and (b) fluorescence spectra of RBA (5 μM) solution upon additions of different amounts of NO (0-40 μM), (c) The plot of fluorescence increments at 585 nm *vs*. the concentration of NO from (b), and (d) Time-dependent fluorescence intensities of 5 μM RBA upon additions of different amounts (0–40 μM) of the NO solution, λ_{ex} = 530 nm.

Furthermore, the kinetics of the reactions of RBA with NO were observed by recording time-dependent fluorescence intensity in the PBS buffer solution. As shown in Fig. 3d, the time-dependent intensities enhance sharply upon additions of NO solutions. For example, most fluorescence increment (>80% of the total signal) is completed within 10 s for 25 μM NO (5 equiv.) solution, comparable to some rapid fluorescent probes.[8, 9, 18f, 21] The observed rate of the sensing reaction is comparable to that of biothiols with NO (within 10 s for 1 mM GSH or Cys with 670 μM NO).[22]

The sensing mechanism

RBA senses NO. Under synthesis condition, we have obtained RBA-NO in a high isolated yield of 60% from the reaction of RBA with saturated NO aqueous solution. To further confirm the efficiency of the reaction, a tracking experiment was carried out by recording ^{1}H NMR spectra of RBA reaction system with different amounts of NO in DMSO-d_6. As shown in Fig. 4, the signals for the protons of the alkyl at amine ($EtOCH_2CH_2$) reveal the conversion from RBA to RBA-NO: disappearance of RBA and appearance of RBA-NO.

In addition, HRMS of the measuring solution of RBA with NO provides an additional evidence for the sensing mechanism (Fig. S2). The *m/z* peak of 537.2236 is accordance with theoretical value of RBA-NO, 537.2244 ($[M+Na]^+$). These results show that RBA can be effectively converted to RBA-NO in the presence of NO.

The DFT calculation for PET mechanism. To explore mechanism for the off-on fluorescence response, the theoretical study was performed by the density functional theory (DFT) method at the B3LYP/6-31+G** level using the package of Gaussian 09 program for proposed PET process from the phenylamine moiety to the BODIPY core. As shown in Fig. S4, the proposed PET process can occur in the probe RBA, and not occur in the sensing product RBA-NO. Hence, the off-on fluorescence response of RBA toward NO via blocking a PET process was clarified.

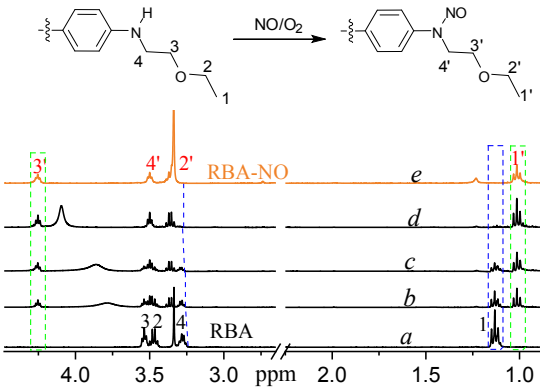

Fig. 4. Partial ^{1}H NMR spectra of RBA before (a) and after additions (b, c, d) of different amounts of NO gas, and neat RBA-NO (e) in DMSO-d_6.

Reaction of GSH with NO. In order to explore the reaction of GSH with NO, NO was bubbled into GSH aqueous solution. A peak of *m/z* 337.0814 was found in the HRMS of mixture of NO and GSH solution, and it is consistent with $[GSNO+H]^+$ (calcd. 337.0813), shown in Fig. S3. This result shows that NO reacts with GSH to form GSNO.

Selectivity

To examine the selectivity of the probe toward NO, fluorescence spectra of RBA in the presence of 40 μM NO or various analytes were recorded after incubation for 30 min. Analytes include metal ions (Ca^{2+}, Mg^{2+}, Zn^{2+}, Fe^{2+}, Cu^{2+}, Fe^{3+}), biomolecules (GSH, Cys, Hcy, ascorbic acid (AA), dehydroascorbic acid (DHA), and methylglyoxal (MGO)), reactive oxygen species (ClO^-, H_2O_2, $OH^\bullet$, $O_2^{\bullet-}$) and reactive nitrogen species (NO_2^-, $ONOO^-$). As shown in Fig 5, the RBA

Journal of Materials Chemistry B Accepted Manuscript

Please do not adjust margins

View Article Online
DOI: 10.1039/D0TB01784A

Published on 19 September 2020. Downloaded by University of Rochester on 9/19/2020 4:01:35 PM.

solution exhibits a turn-on fluorescence response centered at 585 nm only for NO, and no significant change for other analytes (Fig. 5a). These results show high selectivity of RBA for NO over other relevant species.

Furthermore, adding NO into above solutions, their fluorescence spectra were recorded and fluorescence intensities at the peak at 585 nm were shown in Fig. 5b. Under the coexistence of competitive species, fluorescence response of RBA toward NO has no significant change except a reducing agent (Fe^{2+}), biothiols (GSH, Cys and Hcy), and antioxidants (AA and DHA) (Fig. 5b). Above active species would react with NO and/or intercept the sensing reaction of RBA with NO/O_2. Obviously, three biothiols react with NO, resulting in a decrease in the concentration of NO, thus weakening the response signal of RBA to NO. Mayer and co-worker reported that AA inhibited GSNO formation by 67% from GSH and NO.[23] Thus, it is rightful that AA inhibited the RBA-NO from RBA and NO.

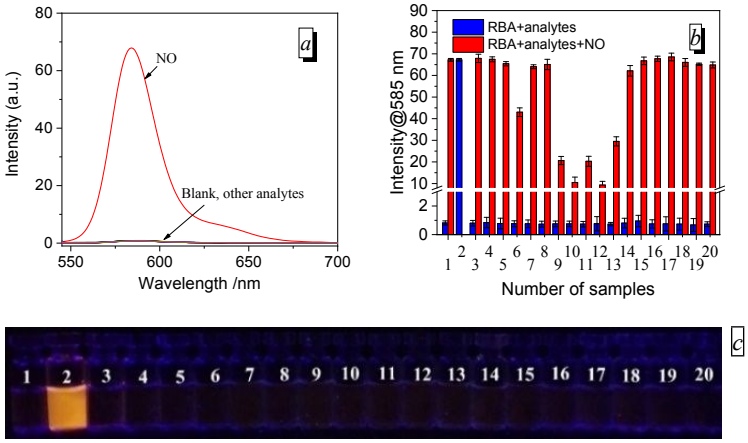

Fig. 5 (a) Fluorescence spectra of 5 μM RBA solution upon addition of 40 μM NO or 400 μM other analytes for 30 min, (b) fluorescence intensities at 585 nm from (a) and (a) + 40 μM NO (except 2), λ_{ex} =530 nm. (c) photo of fluorescence from (a). 1: blank, 2: NO, 3: Ca^{2+}, 4: Mg^{2+}, 5: Zn^{2+}, 6: Fe^{2+}, 7: Cu^{2+}, 8: Fe^{3+}, 9: GSH, 10: Hcy, 11: Cys, 12: AA, 13: DHA, 14: MGO, 15: ClO^-, 16: H_2O_2, 17: $OH^•$, 18: $O_2^{•-}$, 19: NO_2^-, 20: $ONOO^-$.

In addition, the selectivity can be easily observed by naked eyes. As shown in Fig. 5c, RBA solution only gives an orange fluorescence response to NO, and no observable fluorescence was found for other analytes.

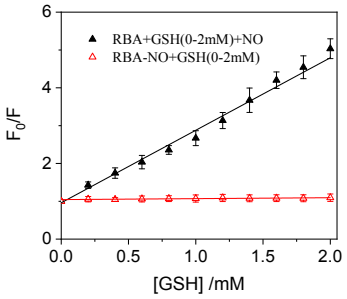

Fig. 6 The fluorescence response at 585 nm (F_0/F) of 5 μM RBA toward NO (40 μM) or 2 μM RBA-NO in the presence of GSH (0–2 mM) for 5 min.

To further investigate the effect of biothiols, fluorescence response of RBA toward NO was observed in the presence of different concentrations of GSH, and compared with the dynamic quenching of the sensing product RBA-NO by GSH in solutions, shown in Fig. S5 and Fig. S6. As shown in Fig. 6, as the concentration of GSH increases to 2 mM, fluorescence intensities at 585 nm of RBA responding NO was quenched more than 80%, and almost no fluorescence change was observed for RBA-NO system. The latter implies that the dynamic quenching between excited RBA-NO and GSH is negligible. Therefore, GSH should compete with RBA for the reaction with NO, leading to a drastic decrease in fluorescence response of RBA toward NO. The level of GSH (2 mM) lies in the range of GSH concentration in cells (1–10 mM), and the sensing reaction of RBA to NO is relative rapid.

Cell-imaging experiments.

cytotoxicity. The cytotoxicity of RBA on HeLa cells was evaluated by employing standard cell viability protocols (MTT assay). HeLa cells were incubated with various concentrations (0–35 μM) of RBA for 24 h (Fig. S7). MTT assays reveal that the survival rates are high, > 90% even at 35 μM. This result shows a very low cytotoxic effect of RBA on HeLa cells.

Cell images of exo- and endogenous NO in living cells. In view of its excellent sensing performance and the low cytotoxicity, RBA was used to visualize NO in living cells. Saturated NO aqueous solution was employed as exogenous NO of living cells. Fig. 7L shows fluorescence images (FI) of HeLa cells stained with 5 μM RBA after additions of different concentrations of NO (0–50 μM). These images exhibit that the emission intensity of cells increases with the concentration of NO. The fluorescence intensities of cells can be obtained from the analysis of cell images with Image J software, and a plot shows clearly that the mean fluorescence intensity increases linearly with NO concentration (Fig. 7R).

Journal of Materials Chemistry B Accepted Manuscript

This journal is © The Royal Society of Chemistry 20xx

Please do not adjust margins

View Article Online
DOI: 10.1039/D0TB01784A

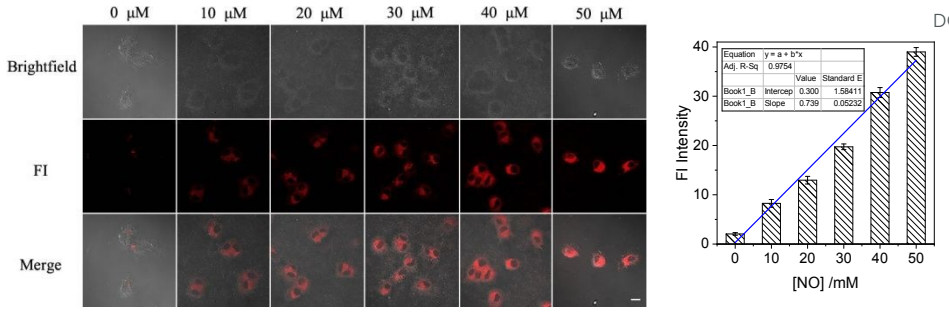

Fig. 7 (Left) Confocal fluorescence images of 5.0 μM RBA loaded HeLa cells incubated with various amounts of NO (0–50 μM) for 10 min. Scale bars, 20 μm. (Right) Plots of fluorescence intensity of 5.0 μM RBA to different concentrations of exogenous NO (0-50 mM) in HeLa cells. The mean values of intensity was analyzed by Image J software.

Furthermore, we tried to use RBA to monitor the change of endogenous NO in living cells. Endogenous NO induced by some stimulants such as lipopolysaccharide (LPS) and interferon-γ (IFN-γ) has been reported on the NO production in Raw 264.7 cells.[24] As shown in Fig. 8, the cells stained with only RBA has no observable fluorescence, and the stimulated cells emit fluorescence, and gradually becomes bright with incubation time in the culture medium containing the stimulants. The fluorescence intensity of cells stimulated displays a good linear relationship with the stimulated time (Fig. S8). Therefore, these observations show that RBA can detect quantitatively exo- ad endogenous NO in living cells.

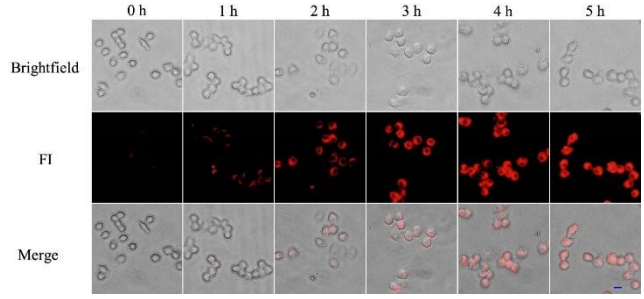

Fig. 8 Fluorescence images of RAW 264.7 cells stimulated with *L*-Arg (0.5 mg/mL), LPS (20 μg/mL) and IFN-γ (400 U/mL) for different time (0-5 h), and then RBA (5 μM) for 1 h. Scale bars, 20 μm.

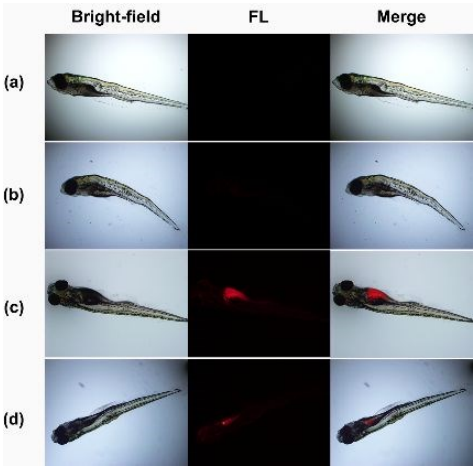

Fig. 9 Fluorescence imaging of RBA toward exo- and endogenous NO generation in Zebrafish. (a) Control fish, (b) feeding only with RBA (5 μM) for 30 min, (c) RBA-feeding fish treated with SNP (1 μM) for another 1 h, or (d) LPS (2 μg/mL) for 3 h, and RBA (5 μM) for another 30 min.

Inspired by above meaningful results for imaging NO in cells, the capability of RBA for imaging NO in zebrafish was evaluated. As shown in Fig. 9, both the control fish and the fish feeding only with RBA exhibits non-fluorescent (Fig. 9ab), while fluorescence from the intestine was observed for the zebrafish supplied with exogenous NO releaser, sodium nitroprusside dihydrate (SNP, Fig. 9c), or endogenous NO stimulant, LPS, shown in Fig. 9d. These results suggest that RBA can be applied to the detection of endo- and exogenous NO in zebrafish.

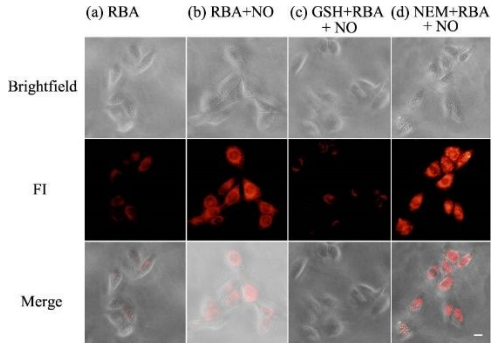

Fig. 10 Fluorescence images of HepG2 cells stained with RBA (5 μM, 1 h) (a) and then treated with NO (50 μM, 15 min) (b), or first incubated with GSH (1 mM, 1 h) (c) or NEM (1 mM, 1 h) (d) and then RBA (5 μM, 1h), finally treated with NO (50 μM, 15 min). Scale bar: 20 μm.

GSH effects on cell-imaging of NO. To investigate the effect of GSH on fluorescence image of RBA to NO, four sets of HepG2 cells were cultured, one set of cells stained with only RBA as a control, other three sets of cells incubated with blank, 1 mM GSH or 1 mM NEM, a thiol scavenger, and then stained with RBA for 1 h and final addition of NO for 15 min, in succession. As shown in Fig. 10, after the addition of NO the cells stained with RBA emit stronger fluorescence over those of the control cells stained only with RBA (Fig. 10ab), and the cells incubated with GSH emit weak fluorescence (Fig. 10c), and the strongest fluorescence from the cells incubated with NEM as a scavenger of thiol group (-SH) (Fig. 10d). These results show that biothiols

Published on 19 September 2020. Downloaded by University of Rochester on 9/19/2020 4:01:35 PM.

Journal of Materials Chemistry B Accepted Manuscript

Please do not adjust margins

View Article Online
DOI: 10.1039/D0TB01784A

Published on 19 September 2020. Downloaded by University of Rochester on 9/19/2020 4:01:35 PM.

can reduce the response of RBA toward NO because it competes to react with NO.

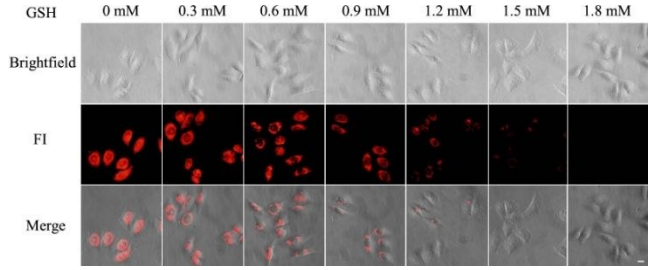

Fig. 11 Fluorescence images of HepG2 cells treated with 1.0 mM NEM for 1 h, 5.0 μM RBA, different concentrations of GSH (0-1.8 mM) for another 1 h, and final 40 μM NO for 10 min. Scale bar, 20 μm.

In order to further investigate the effect of GSH on the fluorescence image, the cells treated with NEM were incubated in the medium containing different concentrations of GSH (0–1.8 mM), and then stained with RBA for cell-imaging of NO. As shown in Fig. 11, the fluorescence of cells becomes gradually weak with GSH concentrations, and the plot of the intensity *vs* the concentration displays a good linear relationship (Fig. S9). This result implies that GSH in live cells reacts with NO, decreasing the response of RBA toward NO.

Therefore, some biomolecules such as biothiols (among them, GSH is the most abundant biothiol in cells, 1–10 mM) that can react with NO would decrease the concentration of NO, and weaken or even eliminate the response signal of a fluorescent probe toward NO, shown in Fig. 12. For chronically elevated or constant NO levels in pathological oxidative stress, reacted biomolecules with NO do not compete with the fluorescent probe, thereby, no interference to the sensing reaction. However, transient bursts NO production in typical of physiological events would react with biomolecules or/and a fluorescent probe. So, the response signal of a fluorescent probe toward NO would decrease even disappear. For this reason, the detection and analysis for the transient NO in live cells is still a challenging task.

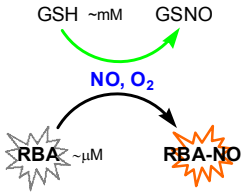

Fig. 12 GSH effect on the sensing reaction of RBA toward NO as a competition reagent.

Conclusions

In summary, we have developed a fluorescent probe, RBA, with a BODIPY as the fluorophore and secondary amine as the reactive site, for NO/GSH. The probe can rapidly sense NO to generate a *N*-nitrosamine RBA-NO with high fluorescence efficiency, in aerobic solutions. RBA displays high selectivity for NO over relevant analytes and high sensitivity (LOD = 10 nM). Moreover, the detection of exo- and endogenous NO has been achieved by bio-imaging experiments. However, there is the interference effect for active biomolecules (reducing reagents) including three biothiols, GSH, Cys and Hcy, via a competition reaction, leading to a large decrease in the response signal. Finally, we have demonstrated that the response intensity of RBA toward NO depend on the level of GSH in living cells by fluorescence cell-imaging.

Experimental section

Material and methods

All chemical reagents were purchased from commercial channels and used without further purification unless otherwise stated. Deionized water for preparation of solutions was purified with a Millipore water system. ^{1}H and ^{13}C NMR spectra were recorded on a Bruker AM 400 MHz and 100 MHz NMR spectrometers, respectively. High-resolution mass spectrometry data were obtained from a FTMS spectrometer or a LC-TOF MS spectrometer. The absorption and fluorescence spectra were recorded at room temperature by using a Shimadzu UV-2450 spectrometer and a Shimadzu RF-5301 PC spectrofluorophotometer, respectively.

Synthesis and Characterization Data of Related Compounds

Synthesis of N-(2-ethoxyethyl)-4-vinylaniline (1). A mixture of 4-vinylaniline (400 mg, 3.36 mmol), 1-bromo-2-ethoxyethane (513 mg, 3.36 mmol), K_2CO_3 (928 mg, 6.72 mmol) and DMF (20 mL) was stirred at 80°C for 12 h, and the TLC showed no raw material. After cooling to room temperature, the mixture was extracted with dichloromethane (100 mL × 3), the organic phases were combined and then washed with water, dried over $MgSO_4$. The filtrate was evaporated to afford crude product, which was purified by silica gel chromatography to give compound **1** as a yellow liquid (250 mg, 40%); ^{1}H NMR (400 MHz, $CDCl_3$, 25°C, TMS): δ = 7.25 (d, J = 7.2 Hz, 2H, Ar-H), 6.61 (dd, J = 17.1, 10.8 Hz, 3H, HC=CH, Ar-H), 5.52 (d, J = 17.7 Hz, 1H, HC=CH), 5.01 (d, J = 10.8 Hz, 1H, Ar-H), 4.11 (s, 1H, NH), 3.64 (t, J = 5.2 Hz, 2H, CH_2), 3.53 (q, J = 7.0 Hz, 2H, CH_2), 3.30 (t, J = 5.2 Hz, 2H, CH_2), 1.22 (t, J = 7.0 Hz, 3H, CH_3) ppm. ^{13}C NMR (100 MHz, $CDCl_3$, 25°C, TMS) δ = 148.0, 136.6, 127.3, 112.9, 109.4, 68.8, 66.4, 43.6, 15.2 ppm. TOFMS (ESI) calcd for $C_{12}H_{18}NO$: 192.1383 $[M+H]^+$, found 192.1377.

Synthesis of tert-Butyl 2-ethoxyethyl(4-vinylphenyl)carbamate (2). $(Boc)_2O$ (315 mg, 1.44 mmol) was dissolved in 1,4-dioxane (5 mL) and then added to the solution of compound **1** (250 mg, 1.31 mmol) in 1,4-dioxane (5 mL). The mixture was stirred under N_2 atmosphere at 85°C for 14 h. The solvent was removed under reduced pressure to get a viscous residue, which was purified by column chromatography (petroleum ether/EtOAc, 3/1, v/v) to afford compound **2** (350 mg, 92%) as a yellow oil; ^{1}H NMR (400 MHz, $CDCl_3$, 25°C, TMS) δ = 7.36 (d, J = 8.1 Hz, 2H, Ar-H), 7.21 (d, J = 7.9 Hz, 2H, Ar-H), 6.69 (dd, J = 17.5, 10.9 Hz, 1H, HC=CH), 5.71 (d, J = 17.6 Hz, 1H, HC=CH), 5.23 (d, J = 10.8 Hz, 1H, Ar-H), 3.78 (t, J = 6.1 Hz, 2H, CH_2), 3.56 (t, J = 6.2 Hz, 2H, CH_2), 3.46 (q, J = 7.0 Hz, 2H, CH_2), 1.44 (s, 9H, CH_3), 1.16 (t, J = 6.9 Hz, 3H, CH_3) ppm. ^{13}C NMR (100 MHz, $CDCl_3$, 25°C, TMS) δ = 154.6, 142.3, 136.2, 135.2, 127.1, 126.4, 113.7, 80.3, 68.0, 66.2, 49.6, 28.3, 15.2 ppm. TOFMS (ESI) calcd for $C_{17}H_{26}NO_3$: 292.1907 $[M+H]^+$, found 292.1902.

Journal of Materials Chemistry B Accepted Manuscript

This journal is © The Royal Society of Chemistry 20xx

Please do not adjust margins

View Article Online DOI: 10.1039/D0TB01784A

Published on 19 September 2020. Downloaded by University of Rochester on 9/19/2020 4:01:35 PM.

Synthesis of 4-(2-Ethoxyethylamino)benzaldehyde (3). Compound **2** (350 mg, 1.20 mmol) was dissolved in 10 mL dry dichloromethane, and bubbled with ozone until the solution becoming light blue at -78°C, and ran for 10 min, and Me_2S (0.3 mL, 0.7mmol) was added, and slowly warmed to room temperature within 30 min. A mixture of dichloromethane/trifluoroacetic acid (1:2) (1.5 mL) was added, and stirred at room temperature for 8 h. The residue was neutralized with $NaHCO_3$ aqueous solution, and the organic phase was dried with $MgSO_4$, and the filtrate was evaporated to afford crude product. The crude product was purified by column chromatography to afford compound **3** as a brown oil (70 mg, 30%); ^{1}H NMR (400 MHz, $CDCl_3$, 25°C, TMS) δ = 9.73 (s, 1H, CHO), 7.70 (d, J = 8.5 Hz, 2H, Ar-H), 6.64 (d, J = 8.3 Hz, 2H, Ar-H), 3.67 (t, J = 5.2 Hz, 2H, CH_2), 3.55 (q, J = 7.1 Hz, 2H, CH_2), 3.38 (t, J = 5.2 Hz, 2H, CH_2), 1.24 (t, J = 7.0 Hz, 3H, CH_3) ppm. ^{13}C NMR (100 MHz, $CDCl_3$, 25°C, TMS) δ = 190.3, 153.3, 132.3, 126.5, 112.0, 68.3, 66.6, 42.8, 15.1 ppm. TOFMS (ESI) calcd for $C_{11}H_{16}NO_2$: 194.1176 $[M+H]^+$, found 194.1176.

Synthesis of 4-(2-(5,5-Difluoro-7-methyl-10-(p-tolyl)-5H-5l4,6l4-dipyrrolo[1,2-c:2',1'-f][1,3,2]diazaborinin-3-yl)vinyl)-N-(2-ethoxyethyl)aniline (RBA). 3,5-Dimethyl BODIPY (438 mg, 1.41 mmol) was added to the solution of 4-(2-ethoxyethylamino) benzaldehyde (300 mg, 1.55 mmol) in toluene (15 mL) and stirred in the presence of piperidine (2 mL, 27.4 mmol) and TsOH (2g, 10.51 mmol) at 145°C for 12 h. The solvent was removed and the crude product was subjected to column chromatography to afford the target compound RBA as a dark blue solid (250 mg, 37%). R_f = 0.48 (PE/EA 1:3). m. p. 128−129°C. ^{1}H NMR (400 MHz, DMSO, 25°C, TMS): δ=7.61 (d, J = 16.4 Hz, 1H, HC=CH), 7.46 (d, J = 7.9 Hz, 2H, Ar-H), 7.39 (dd, J = 12.5, 8.3 Hz, 4H, Ar-H), 7.27 (d, J = 16.1 Hz, 1H, HC=CH), 7.23 (d, J = 4.6 Hz, 1H, Ar-H), 6.90 (d, J = 4.6 Hz, 1H, Ar-H), 6.69 (d, J = 8.6 Hz, 2H, Ar-H), 6.65 (d, J = 3.9 Hz, 1H, Ar-H), 6.52 (t, J = 5.5 Hz, 1H, NH), 6.37 (d, J = 3.9 Hz, 1H, Ar-H), 3.54 (t, J = 5.6 Hz, 2H, CH_2), 3.47 (q, J = 7.0 Hz, 2H, CH_2), 3.28 (t, J = 5.7 Hz, 2H, CH_2), 2.55 (s, 3H, CH_3), 2.42 (s, 3H, CH_3), 1.13 (t, J = 7.0 Hz, 3H, CH_3) ppm. ^{13}C NMR (100 MHz, DMSO, 25°C, TMS) δ = 157.7, 154.6, 153.0, 151.3, 140.7, 140.3, 138.8, 135.7, 133.7, 132.4, 131.4, 131.3, 130.7, 130.0, 129.6, 127.5, 125.3, 123.9, 118.5, 118.2, 112.7, 112.5, 111.7, 68.7, 66.0, 42.9, 21.4, 15.6, 14.9 ppm. TOFMS (ESI) calcd for $C_{29}H_{31}N_3OBF_2$: 486.2523 $[M+H]^+$, found 486.2518.

Synthesis of N-(4-(2-(5,5-Difluoro-7-methyl-10-(p-tolyl)-5H-5l4,6l4-dipyrrolo[1,2-c:2',1'-f][1,3,2]diazaborinin-3-yl)vinyl)phenyl)-N-(2-ethoxyethyl)nitrous amide (RBA-NO). A stock solution of NO in water was added to a solution of RBA (50 mg, 0.103 mmol) in EtOH (2 mL), and stirred for 5 min in room temperature. The reaction mixture extracted with dichloromethane (20 mL × 3), and the organic phases were combined, dried over $MgSO_4$. Evaporation and purification of the residue by silica gel flash chromatography (EtOAc/PE = 1:3) gave RBA-NO as a bluish violet solid (30 mg, 60%). R_f = 0.63 (PE/EA 1:3), mp 148−149°C. ^{1}H NMR (400 MHz, DMSO, 25°C, TMS): δ = 7.80-7.74 (m, 5H, HC=CH, Ar-H), 7.58 (d, J = 16.7 Hz, 1H, HC=CH), 7.51 (d, J = 7.9 Hz, 2H, Ar-H), 7.41 (d, J = 7.8 Hz, 2H, Ar-H), 7.28 (d, J = 4.5 Hz, 1H, Ar-H), 6.95 (d, J = 4.4 Hz, 1H, Ar-H), 6.85 (d, J = 4.2 Hz, 1H, Ar-H), 6.52 (d, J = 4.1 Hz, 1H, Ar-H), 4.26 (t, J = 5.5 Hz, 2H, CH_2), 3.50 (t, J = 5.5 Hz, 2H, CH_2), 3.36 (q, J = 7.0 Hz, 2H, CH_2), 2.61 (s, 3H, CH_3), 2.44 (s, 3H, CH_3), 1.01 (t, J = 7.0 Hz, 3H, CH_3) ppm. ^{13}C NMR (100 MHz, DMSO, 25°C, TMS) δ = 157.4, 154.3, 142.5, 141.6, 140.9, 136.5, 135.4, 135.4, 134.5, 130.9, 130.9, 129.7, 128.6, 121.0, 120.7, 118.9, 117.6, 66.0, 65.8, 44.3, 21.5, 15.4, 15.1 ppm. TOFMS (ESI) calcd for $C_{29}H_{29}N_4O_2BF_2Na$: 537.2244 $[M+Na]^+$, found 537.2285.

Preparation of Solution Samples

All measurement solutions were prepared with phosphate buffer (0.1 M, pH 7.4)/EtOH solution mixture (v/v, 65:35), and all measurements were performed at room temperature. NO saturated aqueous solution was prepared by bubbling NO gas into a NaOH solution to eliminate NO_2 generated from the reaction of NO and O_2, then into deoxygenated deionized water for 30 min. The concentration of the NO saturated solution is 1.9 mM.[25] Various analytes were prepared in the terms of methods as follows. NO_2^- and hydrochlorite (ClO^-) solutions were from aqueous solutions of $NaNO_2$ and NaClO freshly prepared, respectively. Peroxynitrite ($ONOO^-$) solution was prepared according to literature,[26] and its concentration was estimated in terms of the extinction coefficient of 1670 $M^{-1}cm^{-1}$ at 302 nm. Superoxide ($O_2^{\bullet-}$) solution was prepared through adding KO_2 (1 mg) to dry dimethyl sulfoxide (1 mL) and stirring vigorously for 10 min. Hydroxyl radical ($HO^{\bullet}$) was generated in situ by the Fenton reaction. H_2O_2 solution was obtained by dilution of commercial H_2O_2 solution with deionized water.

The theoretical calculation for the PET process

All theoretical calculations were carried out by using the package of Gaussian 09 program.[27] Geometry optimizations for molecules were carried out using density functional theory (DFT) at the level of B3LYP/6-31+G**. Then, solvent effects of acetonitrile were performed by the polarizable continuum model (PCM)[28] with time-dependent density functional theory (TDDFT) calculations.

Fluorescence imaging experiments.

Cell culture and MTT assay. The cytotoxicity was evaluated by MTT assay. HeLa cells were cultured in Dulbecco's modified Eagle's medium (DMEM) in 96-well microplates at 37°C under 5% CO_2 and 95% air for 12 h. The medium was next replaced by fresh medium containing various concentrations of RBA (0-35 μM). Each concentration was tested in three replicates. Cells were rinsed twice with phosphate buffer saline 24 h later and incubated with 10 μL of 5 mg/mL MTT reagent for 4 h at 37°C. 150 μL DMSO was then added to dissolve formazan. The absorbance at 570 nm was measured in a microplate reader. Cell viability (%) was calculated according to following equation: Viability = (mean Abs. of treated wells/mean Abs. of control wells) ×100%.

Cells imaging experiments. HeLa, RAW264.7 and HepG2 cells were employed for cell imaging experiments. The cell imaging experiments were performed by laser scanning confocal fluorescence microscope (Zeiss LSM 880 with Airyscan) for HeLa cells or IX71 fluorescence microscope (Olympus, Japan) for RAW264.7 and HepG2 cells. The HeLa cells were stained initially with 5 μM RBA for 1 h, washing with PBS buffer for 3 times, and then 0−50 μM NO stock solution was added to the incubation medium, and incubated for 10 min. Finally, these cells were fixed for fluorescence imaging. For other experiments, RAW264.7 or HepG2 cells with RBA were incubated in the presence of GSH or *N*-ethylmaleimide (NEM), washing with PBS buffer for 3 times, and

Journal of Materials Chemistry B Accepted Manuscript

Please do not adjust margins

then NO stock solution was added for incubation for 10 min. Live cells were washed with PBS buffer for 3 times and then adding fresh incubation medium for cell-imaging.

Imaging of NO in Zebrafish. For visualization of NO in zebrafish, 6-day-old zebrafish embryos were incubated within fresh E3 culture medium containing RBA (5 μM) for 30 min, then SNP (1 μM) for another 1h for exogenous NO experiment. Another group of fishes were treated with LPS (2 μg/mL) for 3 h, then RBA (5 μM) for another 30 min for endogenous NO experiment. After that, the fish were washed three times with E3 media and observed on an Olympus IX71 inverted fluorescence microscope.

Conflicts of interest

There are no conflicts to declare.

Acknowledgements

Financial support of the National Natural Science Foundation of China (No. 21772188) is gratefully acknowledged.

Notes and references

1 S. H. Snyder, *Science*, 1992, **257**, 494; S. Jasid, M. C. Simontacchi, G. Bartoli and S. Puntarulo, *Plant Physiol.*, 2006, **142**, 1246; D. Fukumura, S. Kashiwagi and R. K. Jain, *Nat. Rev. Cancer*, 2006, **6**, 521; C. Coletta, A. Papapetropoulos, K. Erdelyi, G. Olah, K. Modis, P. Panopoulos, A. Asimakopoulou, D. Gero, I. Sharina, E. Martin and C. Szabo, *Proc. Natl. Acad. Sci. U.S.A.*, 2012, **109**, 9161.

2 S. Taysi, C. Uslu, F. Akcay and M. Y. Sutbeyaz, *Surg. Today*, 2003, **33**, 651; G. P. Biro, *Curr. Drug Discov. Technol.*, 2012, **9**, 194-203; D. Y. Choi, Y. J. Lee, J. T. Hong and H. J. Lee, *Brain Res. Bull.*, 2012, **87**, 144; S. Yuan, R. P. Patel and C. G. Kevil, *Am. J. Physiol.: Lung Cell. Mol. Physiol.*, 2015, **308**, L403.

3 D. D. Thomas, L. A. Ridnour, J. S. Isenberg, W. Flores-Santana, C. H. Switzer, S. Donzelli, P. Hussain, C. Vecoli, N. Paolocci, S. Ambs, C. A. Colton, C. C. Harris, D. D. Roberts and D. A. Roberts, *Wink, Free Radicals Biol. Med.*, 2008, **45**, 18; A. Martínez-Ruiz, S. Cadenas and S. Lamas, *Free Radicals Biol. Med.*, 2011, **51**, 17.

4 X. Chen, X. Tian, I. Shin and J. Yoon, *Chem. Soc. Rev.*, 2011, **40**, 4783; Y. Yang, Q. Zhao, W. Feng and F. Li, *Chem. Rev.*, 2013, **113**, 192.

5 H. Li and A. Wan, *Analyst*, 2015, **140**, 7129; X. Zhou, S. Lee, Z. Xu and J. Yoon, *Chem. Rev.*, 2015, **115**, 7944; X. Chen, F. Wang, J. Y. Hyun, T. Wei, J. Qiang, X. Ren, I. Shin and J. Yoon, *Chem. Soc. Rev.*, 2016, **45**, 2976.

6 H. Kojima, Y. Urano, K. Kikuchi, T. Higuchi, Y. Hirata and T. Hirata, *Angew. Chem. Int. Ed.*, 1999, **38**, 3209.

7 M. H. Lim and S. J. Lippard, *J. Am. Chem. Soc.*, 2005, **127**, 12170.

8 J. Miao, Y. Huo, X. Lv, Z. Li, H. Cao, H. Shi, Y. Shi and W. Guo, *Biomaterials*, 2016, **78**, 11.

9 Y. Yang, S. K. Seidlits, M. M. Adams, V. M. Lynch, C. E. Schmidt, E. V. Anslyn and J. B. Shear, *J. Am. Chem. Soc.*, 2010, **132**, 13114.

10 T.-W. Shiue, Y.-H. Chen, C.-M. Wu, G. Singh, H.-Y. Chen, C.-H. Hung, W.-F. Liaw and Y.-M. Wang, *Inorg. Chem.*, 2012, **51**, 5400.

11 H.-L. Wang, F.-T. Liu, A.-X. Ding, S.-F. Ma, L. He, L. Lin and Z.-L. Lu, *Spectrochim. Acta Part A*, 2016, **169**, 1.

12 C. Sun, W. Shi, Y. Song, W. Chen and H. Ma, *Chem. Commun.*, 2011, **47**, 8638.

13 I A. S. M. Islam, R. Bhowmick, K. Pal, A. Katarkar, K. Chaudhuri, and M. Ali, *Inorg. Chem.*, 2017, **56**, 4324; L. Chen, D. Wu and J. Yoon, *Sens. Actuators, B.*, 2018, **259**, 347. A. S. M.Islam, R. Bhowmick, B. C. Garain, A. Katarkar and M. Ali, *J. Org. Chem.*, 2018, **83**, 21, 13287.

14 (a) Z. Mao, H. Jiang, Z. Li, C. Zhong, W. Zhang and Z. Liu, *Chem. Sci.*, 2017, **8**, 4533; (b) Z. Mao, H. Jiang, X. Song, W. Hu and Z. Liu, *Anal. Chem.*, 2017, **89**, 9620; (c) C. J. Reinhardt, E. Y. Zhou, M. D. Jorgensen, G. Partipilo and J. Chan, *J. Am. Chem. Soc.*, 2018, **140**, 1011; (d) Y. Huo, J. Miao, J. Fang, H. Shi, J. Wang and W. Guo, *Chem. Sci.*, 2019, **10**, 145; (e) Z. Yu, J. Zhou, X. Dong, W. Zhao and Z. Chen, *Anal. Chim. Acta*, 2019, **1067**, 88; (f) Y. Zuo, X. Wang, Z. Gou and W. Lin, *Chem. Commun.*, 2020, **56**, 1121.

15 J. S. Stamler, D. I. Simon, J. A. Osborne, M. E. Mullins, O. Jaraki, T. Michel, D. J. Singel, and J. Loscalzo, *Proc. Natl. Acad. Sci. USA*, 1992, **89**, 444; D. T. Hess, A. Matsumoto, S. O. Kim, H. E. Marshall and J. S. Stamler, *Nat. Rev. Mol. Cell Biol.*, 2005, **6**, 150.

16 M. Kelm, *Biochim. Biophys. Acta, Bioenerg.*, 1999, **1411**, 273.

17 U. Seneviratne, L. C. Godoy, J. S. Wishnok, G. N. Wogan and S. R. Tannenbaum, *J. Am. Chem. Soc.*, 2013, **135**, 7693.

18 (a) Z. Mao, W. Feng, Z. Li, L. Zeng, W. Lv and Z. Liu, *Chem. Sci.*, 2016, **7**, 5230; (b) Y. Huo, J. Miao, Y. Li, Y. Shi, H. Shi and W. Guo, *J. Mater. Chem. B*, 2017, **5**, 2483; (c) P. Zhang, Y. Tian, H. Liu, J. Ren, H. Wang, R. Zeng, Y. Long and J. Chen, *Chem. Commun.*, 2018, **54**, 7231; (d) Q. Han, J. Liu, Q.-T. Meng, Y.-L. Wang, H. Feng, Z.-Q. Zhang, Z. P. Xu and R. Zhang, *ACS Sens.*, 2019, **4**, 309; (e) W.-L. Jiang, Y. Li, H.-W. Liu, D.-Y. Zhou, J. Ou-Yang, L. Yi and C.-Y. Li, *Talanta*, 2019, **197**, 436; (f) C. Li, W. -J.Tang, W. Feng, C. Liu and Q.-H. Song, *Anal. Chim. Acta*, 2020, **1096**, 148.

19 Y. Chen, L. Wan, D. Zhang, Y. Bian and J. Jiang, *Photochem. Photobiol. Sci.*, 2011, **10**, 1030.

20 D. Magde, J. H. Brannon, T. L. Cremers and J. Olmsted, *J. Phys. Chem.*, 1979, **83**, 696.

21 X. Chen, L. Sun, Y. Chen, X. Cheng, W. Wu, L. Ji and H. Chao, *Biomaterials*, 2015, **58**, 72; C.-B. Huang, J. Huang and L. Xu, *RSC Adv.*, 2015, **5**, 13307; H. Li, D. Zhang, M. Gao, L. Huang, L. Tang, Z. Li, X. Chen and X. Zhang, *Chem. Sci.*, **2017**, **8**, 2199; C.-G. Dai, J.-L. Wang, Y.-L. Fu, H.-P. Zhou and Q.-H. Song, *Anal. Chem.*, 2017, **89**, 10511.

22 D. A.Wink, R. W.Nims, J. F. Derbyshire, D. Christodoulou, I. Hanbauer, G. W. Cox, F. Laval, J. Laval, J. A. Cook, M. C. Krishna, W. G. DeGraff and J. B. Mitchell, *Chem. Res. Toxicol.*, 1994, **7**, 519; M. Keshive, S. Singh, J. S. Wishnok, S. R. Tannenbaum and W. M. Deen, *Chem. Res. Toxicol.*, 1996, **9**, 988.

23 A. Schrammel, A. C. F. Gorren, K. Schmidt, S. Pfeiffer and B. Mayer, *Free Radic. Biol. Med.*, 2003, **34**, 1078.

24 T. R. M. da Silva, J. R. de Freitas, Q. C. Silva, C. P. Figueira, E. Roxo, S. C. Leao, L. A. R. de Freitas and P. S. T. Veras, *Infect. Immun.*, 2002, **70**, 5628; H. Yuan, C. N. Perry, C. Huang, E. Iwai-Kanai, R. S. Carreira, C. C. Glembotski and R. A. Gottlieb, *Am. J. Physiol.-Heart Circ. Physiol.*, 2009, **296**, H470.

25 J. Hartung, *Chem. Rev.*, 2009, **109**, 4500.

26 R. M. Uppu and W. A. Pryor, *Anal. Biochem.*, 1996, **236**, 242.

27 Frisch, M. J. et al. *Gaussian 09, Revision C.01, Gaussian, Inc., Wallingford CT,* 2010.

28 C. Lee, W. Yang and R. G. Parr, *Phys. Rev. B: Condens. Matter Mater. Phys.*, 1988, **37**, 785.

View Article Online DOI: 10.1039/D0TB01784A

Published on 19 September 2020. Downloaded by University of Rochester on 9/19/2020 4:01:35 PM.

Journal of Materials Chemistry B Accepted Manuscript

This journal is © The Royal Society of Chemistry 20xx

Please do not adjust margins

View Article Online
DOI: 10.1039/D0TB01784A

Table of Contents Entry:

Glutathione effects on the sensing reaction toward nitric oxide in live cells

Published on 19 September 2020. Downloaded by University of Rochester on 9/19/2020 4:01:35 PM.

Journal of Materials Chemistry B Accepted Manuscript